ACS chemical biology

Articles

pubs.acs.org/acschemicalbiology

# Calcium-Dependent Ligand Binding and G-protein Signaling of Family B GPCR Parathyroid Hormone 1 Receptor Purified in Nanodiscs

Nivedita Mitra,[†,§] Yuting Liu,[†,§] Jian Liu,[†] Eugene Serebryany,[†] Victoria Mooney,[†] Brian T. DeVree,[‡] Roger K. Sunahara,[‡] and Elsa C. Y. Yan*[,†]

[†]Department of Chemistry, Yale University, New Haven, Connecticut 06520, United States

[‡]Department of Pharmacology, University of Michigan Medical School, Ann Arbor, Michigan 48109, United States

Supporting Information

**ABSTRACT:** GPCRs mediate intracellular signaling upon external stimuli, making them ideal drug targets. However, little is known about their activation mechanisms due to the difficulty in purification. Here, we introduce a method to purify GPCRs in nanodiscs, which incorporates GPCRs into lipid bilayers immediately after membrane solubilization, followed by single-step purification. Using this approach, we purified a family B GPCR, parathyroid hormone 1 receptor (PTH1R), which regulates calcium and phosphate homeostasis and is a drug target for osteoporosis. We demonstrated that the purified PTH1R in nanodiscs can bind to PTH(1-34) and activate G protein. We also observed that $Ca^{2+}$ is a weak agonist of PTH1R, and $Ca^{2+}$ in millimolar concentration can switch PTH(1-34) from an inverse agonist to an agonist. Hence, our results show that nanodiscs are a viable vehicle for GPCR purification, enabling studies of GPCRs under precise experimental conditions without interference from other cellular or membrane components.

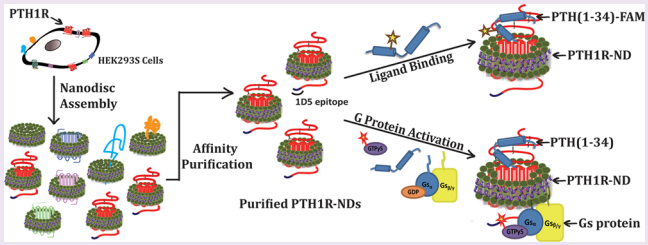


Integral membrane proteins can be challenging to purify and study. G-protein-coupled receptors (GPCRs) are the largest class of integral membrane proteins found in the human genome and are represented by approximately 1000 genes.[1] These 7-helical-transmembrane proteins constitute a major portal for intercellular communication. Upon binding to their ligand on their extracellular or transmembrane domain, GPCRs transduce a signal *via* conformational changes to the cytoplasmic side, which then couples with G-proteins to start signaling cascades. Based on GPCRs' function and amino acid sequence, they are classified into 5 families (A–E), of which families A, B, and C are best studied with respect to their ligand binding, function, and G-protein coupling.[2] However, most biophysical and activation mechanism studies have been performed only on family A GPCRs, using model systems, such as rhodopsin and $\beta_2$-adrenergic receptor.[3−9] These studies reveal precise information about roles of amino acids and helical movements in the transmembrane region upon activation. Such detailed information is unavailable for families B and C, largely due to difficulty in purifying them while retaining their activity for biophysical studies. Apart from reasons such as low cellular expression levels, the difficulty in purifying GPCRs can also arise from their labile membrane-embedded hydrophobic domains, which require detergents for solubilization and extraction from the plasma membrane. Solubilization is a critical step in the purification procedure, where the target GPCR is separated from the membrane lipids of the expressing cell systems. Traditionally, once GPCRs are separated from cell membranes with a detergent, all subsequent purification steps are also done in detergent.[10] The purified GPCRs are then either stored in detergent or reconstituted into lipid environments.[11] Such prolonged exposure to detergent could be an additional contributing factor in denaturation of GPCRs during purification.

Here, we propose that minimizing detergent contact with GPCRs can preserve their structure and stabilize them. One way to achieve minimal detergent contact is by using nanodiscs. Nanodiscs, also referred to as NABBs (Nanoscale Apolipoprotein Bound Bilayers),[12] are a discoidal form of HDL (High-density Lipoproteins). They are composed of nanometer-sized lipid bilayers surrounded by two alpha helical membrane scaffold proteins (MSP).[13] MSPs are modified versions of apolipoprotein A.[14] Nanodics were first characterized by the Sligar group.[14] Because nanodiscs mimic a membrane, they could be ideal vehicles for stabilization of transmembrane proteins. A recent study showed that MSP can be replaced by polymers to form particles called Lipodisq.[15] Because nanodiscs mimic a membrane, they could be ideal vehicles for stabilization of transmembrane proteins. In this study, we use nanodiscs formed by the MSP MSP1E3D1 to purify GPCRs. We incorporate our target GPCRs into nanodiscs immediately after solubilization from the expression system to minimize

**Received:** August 31, 2012
**Accepted:** December 11, 2012
**Published:** December 13, 2012

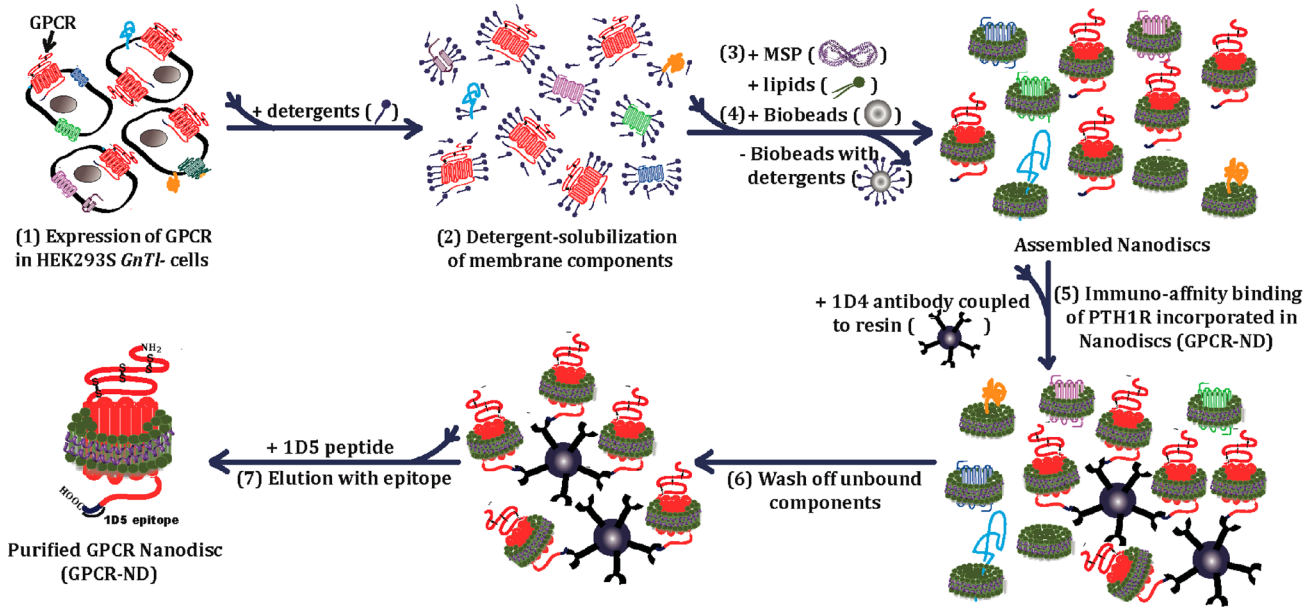


**Figure 1.** Schematic of purification of a family B GPCR in nanodiscs. The purification procedure includes (1) expression of a family B GPCR in a mammalian expression system, (2) solubilization of membrane components of the expression system using detergent, (3) incubation of solubilized membrane components with phospholipid and the membrane scaffold protein, MSP1E3D1, (4) addition of Bio-Beads to remove detergent by physical adsorption to induce formation of nanodiscs containing membrane proteins, (5) immuno-affinity binding of the GPCR incorporated in nanodiscs (GPCR-ND) to antibody-conjugated resin, (6) washing resins bound with GPCR-ND, and (7) elution with epitope to yield purified GPCR-ND.

detergent contact and purify the receptors by single-step affinity chromatography while the receptors are in the lipid environment of nanodiscs (Figure 1).

Although nanodiscs have been applied to study membrane proteins,[16−23] they have not been used as a vehicle to purify GPCRs. Previous studies have shown that when membrane proteins are incorporated into nanodiscs, they display improved stability and activity.[12,24] Nanodiscs were used to incorporate rhodopsin, $\beta_2$-adrenergic receptor, $\mu$-opioid receptor, and CCR5 for examining their interactions with G-proteins.[12,19,25−27] Moreover, rhodopsin incorporated into nanodiscs can couple with downstream signaling proteins, including rhodopsin kinase and arrestin-1.[28,29] However, in these previous studies, GPCRs were incorporated into nanodiscs after being purified in detergent. Although nanodiscs have been applied to directly purify a membrane-anchored protein, cytochrome P450 monooxygenase,[30] nanodiscs have never been used as a means for purifying integral membrane proteins, such as GPCRs.

Here, we use parathyroid hormone 1 receptor (PTH1R), of which the purification in detergent has been reported, as a model system to establish our proposed nanodisc methodology for purifying GPCRs. The receptor belongs to family B GPCRs. To date, there have been a small number of successful cases of purifying family B GPCRs, which include pituitary adenylate cyclase-activating peptide receptor purified from bovine brain[31] and insect cells;[32] PTH1R purified from COS-7 cells,[33] HEK293S cells,[34] and *E. coli*;[35] glucagon-like peptide 1 receptor purified from both *E. coli*[36] and insect cells;[37] and two other receptors, corticotrophin-releasing factor receptors 1 and 2$\beta$, obtained using cell-free expression methods.[38] In this study, we choose PTH1R as our target receptor, because it has been shown to be stable in detergents. Thus, it is a good model system for establishing and standardizing the purification protocol.

PTH1R is expressed in osteoblasts in bone and tubule epithelial cells in the kidney and is a target for osteoporosis treatment.[39] It has two endogenous ligands, parathyroid hormone 1 (PTH) and parathyroid hormone-related protein (PTHrP). It regulates calcium and phosphate homeostasis in blood and extracellular fluids upon binding to PTH, and subsequent coupling with either $G_s$ or $G_q$, which activates the adenylyl cyclase or phospholipase C signaling pathways, respectively.[39] Association of PTH1R with PTHrP is important in the development of organs, such as bone, heart, mammary glands, and other tissues.[39−41] A truncated version of PTH, PTH(1-34) that has the first 34 amino acids, maintains the same functions as the full-length ligand.[39] Paradoxically, while activation of PTH1R by PTH or PTH(1-34) results in bone resorption (release of $Ca^{2+}$ from bone), intermittent injection of PTH(1-34) can enhance bone formation, and is an FDA-approved treatment for osteoporosis.[42]

In this study, we extracted PTH1R in nanodiscs and characterized the properties and functions of the purified PTH1R incorporated in nanodiscs (PTH1R-ND). We used fluorescence anisotropy to study the binding of fluorescently labeled PTH(1-34) to the purified PTH1R-ND and obtained binding constants at various $Ca^{2+}$ concentrations. We also used a fluorescently labeled nonhydrolyzable GTP analogue to examine the ability of PTH1R-ND to activate G-protein ($G_s$) in response to the binding of PTH(1-34).

Our studies reveal that both ligand binding and G-protein activation by PTH1R-ND strongly depend on $Ca^{2+}$ concentration. In particular, $Ca^{2+}$ at millimolar concentrations can switch PTH(1-34) from inverse agonist to agonist, and $Ca^{2+}$ alone can weakly activate PTH1R under the conditions of our experiments. These results demonstrate that nanodiscs can be a viable vehicle for GPCR purification, which enables precise control of experimental conditions, such as $Ca^{2+}$ concentration,


dx.doi.org/10.1021/cb300466n | *ACS Chem. Biol.* 2013, 8, 617−625

for functional characterization that would be difficult in cells or membrane preparations.

## RESULTS

**Purification of PTH1R in Nanodiscs.** The purification process starts with expressing a full-length PTH1R tagged with the 1D5 epitope (TETSQVAPA) in HEK293S cells (Figure 1). Membrane fractions of the PTH1R expressing cells were isolated (described in Supplementary Methods) and then solubilized using *n*-dodecyl-*β*-D-maltopyranoside (DDM). The solubilized membrane fractions were incubated with 1-palmitoyl-2-oleoyl-*sn*-glycero-3-phosphocholine (POPC) and MSP1E3D1. Subsequently, Bio-Beads were added to remove DDM by physical adsorption. Upon removal of DDM, nanodiscs form spontaneously, which incorporate POPC and the membrane components of the HEK293S cells, including the overexpressed 1D5-tagged PTH1R. Then, 1D4 antibody coupled resin was added to the assembly mix to specifically bind PTH1R incorporated in nanodiscs (PTH1R-ND). The resin was washed, and the bound PTH1R-ND was eluted using the 1D5 peptide. We established this protocol through several rounds of optimization of various experimental parameters, including the lipid to detergent ratio, the MSP1E3D1 to membrane protein ratio, the MSP1E3D1 to lipid ratio, and the amount of Bio-Beads, which are detailed in the Supporting Information. Using this optimized protocol to purify PTH1R, we obtained a yield ranging roughly from 0.05 to 0.2 $\mu$g of PTH1R per 10-cm plate of HEK293S cells (Supplementary Figure 1).

**Characterization of Physical Properties of PTH1R-ND.** Next, we characterized the size, size distribution, and purity of PTH1R-ND. We used size exclusion chromatography to measure the Stokes diameter of PTH1R-ND. The gel filtration profile showed a major peak at 10.7 mL (Figure 2a). Calibration with protein standards (vertical bars on the top of the elution profile) confirmed that this peak corresponded to a Stokes diameter of 12.5 nm. We would like to point out here that the Stokes diameter assumes a spherical shape of the particle being measured, whereas nanodiscs are disc-shaped. The profile also contained an earlier eluting peak, representing aggregates that are too large for the column to resolve. To further characterize the size and size distribution, we used transmission electron microscopy (TEM). We took several EM images, and each image displayed roughly 200 particles (Figure 2b), of which most are homogeneous with a diameter of ~15 nm (Figure 2b, lower panel). A few particles appeared to be 2–3 times larger than the rest, which is consistent with the gel filtration profile. We also ran a SDS-PAGE gel and stained it with Coomassie blue. The gel contained two main bands with apparent molecular weights of 28 and 75 kD, corresponding to MSP1E3D1 and PTH1R, respectively (Figure 2c).

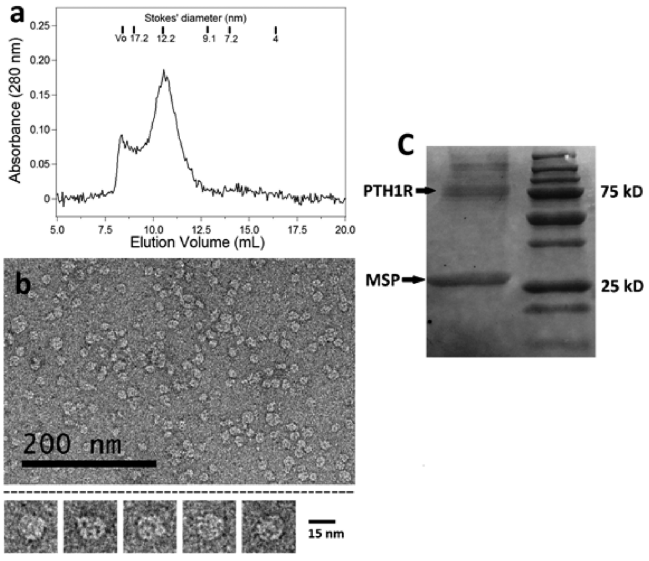


**Figure 2.** Characterizations of physical properties of PTH1R-ND. (a) Size exclusion chromatogram of purified PTH1R-ND. (b) Transmission electron micrograph of negatively stained purified PTH1R-ND. Lower panel: images of PTH1R-ND with a scaling bar of 15 nm. (c) Coomassie-stained SDS-PAGE of the purified nanodisc preparation showing two major bands corresponding to MSP1E3D1 (~28 kD) and PTH1R (~75 kD).

**Effect of $Ca^{2+}$ on Ligand Binding of PTH1R-ND.** Next, we examined the ligand binding activity of PTH1R-ND using fluorescence anisotropy and observed an effect of $Ca^{2+}$ concentration on the ligand affinity. We designed a fluorescently labeled ligand, PTH(1-34)-FAM, which is labeled with 5(6)-carboxyfluorescein (FAM) at Lys13 (Figure 3a). The concentration of PTH(1-34)-FAM was fixed at 50 nM and titrated with freshly prepared PTH1R-ND in Buffer A (20 mM Tris at pH 7.4, 150 mM NaCl, 100 $\mu$M EDTA, and 3 mM $MgCl_2$). In the presence of 15 mM $Ca^{2+}$, the anisotropy of PTH(1-34)-FAM increased with an increase in PTH1R-ND concentration (Figure 3b). This increase is due to the binding

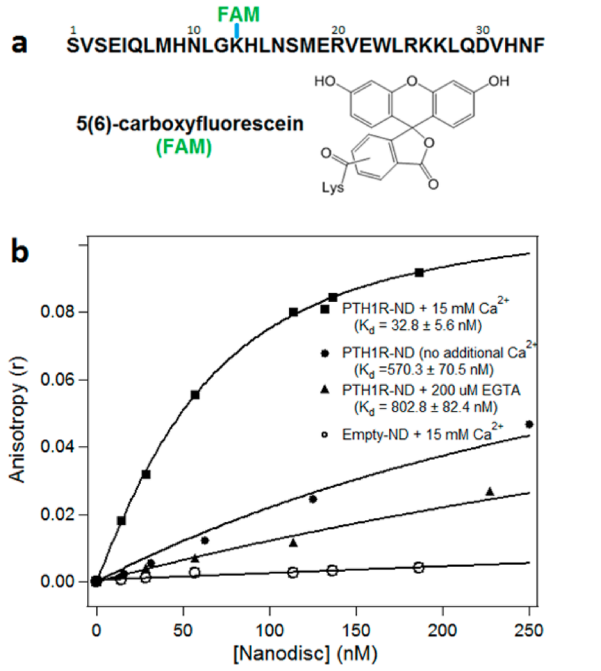


**Figure 3.** Ligand-binding activity assay using fluorescence anisotropy. (a) PTH(1-34)-FAM peptide: (upper) sequence of PTH(1-34) conjugated to 5(6)-carboxyfluorescein (FAM) at Lys13 and (lower) structure of FAM. (b) Titration of PTH(1-34)-FAM (50 nM) with four nanodisc samples: (■) PTH1R-ND with 15 mM $Ca^{2+}$, (●) PTH1R-ND without added $Ca^{2+}$, (▲) PTH1R-ND with 200 $\mu$M EGTA, and (○) nanodiscs containing no PTH1R (empty-ND) with 15 mM $Ca^{2+}$. Indicated $Ca^{2+}$ and EGTA concentrations are final. Buffer A: 20 mM Tris (pH 7.4), 150 mM NaCl, 100 $\mu$M EDTA, and 3 mM $MgCl_2$.


dx.doi.org/10.1021/cb300466n | ACS Chem. Biol. 2013, 8, 617–625

of PTH(1-34)-FAM onto PTH1R-ND, resulting in a slower rotational diffusion. We analyzed the titration curve using a binding model (Supporting Information) to obtain the dissociation constant ($K_d$), which was reproducible over four experiments with an average value of 32.8 ± 5.6 nM. When no additional $Ca^{2+}$is added, the increase in anisotropy of PTH(1-34)-FAM with increase in PTH1R-ND concentration is much smaller. The $K_d$ averaged from three independent measurements is 570.3 ± 70.5 nM. When empty nanodiscs (empty-ND) are used instead of PTH1R-ND, there is no change in anisotropy even in the presence of 15 mM $Ca^{2+}$, suggesting that binding of PTH(1-34)-FAM is specific to PTH1R. Altogether, the results suggest that the purified PTH1R-ND can bind to PTH(1-34)-FAM. The results also show that ligand binding is highly $Ca^{2+}$-dependent and the presence of 15 mM $Ca^{2+}$ increases the association constant of PTH(1-34)-FAM to PTH1R-ND by an order of magnitude.

**Lower Affinity of Ligand Binding under a $Ca^{2+}$-Depleting Condition.** We also examined the binding of PTH(1-34)-FAM to PTH1R-ND under a $Ca^{2+}$-depleting condition, *i.e.*, in the presence of 200 μM EGTA. EGTA is used to remove residual $Ca^{2+}$ in the buffer that was introduced as impurity from the buffer components (Tris-HCl, NaCl, and $MgCl_2$). $Ca^{2+}$ impurities on bottle labels were specified as ≤10 mg/kg for Tris-HCl, 0.002% for NaCl, and 0.01% for $MgCl_2$. The residual $Ca^{2+}$ in the buffer is expected to be less than 6 μM. Indeed, the concentration of $Ca^{2+}$ in our buffer was measured using the inductively coupled plasma optical emission spectrometry (ICP-OES) method by Robertson Microlit Laboratories and found to be undetectable with a specified detection limit of 1 ppm (~25 μM). Thus, addition of 200 μM EGTA is expected to remove all residual $Ca^{2+}$. Under this condition, a titration of PTH(1-34)-FAM (50 nM) with PTH1R-ND still leads to an increase in PTH(1-34)-FAM anisotropy (Figure 3b). However, the increase is relatively small compared to other conditions shown in Figure 3. The $K_d$ is measured to be 802.8 ± 82.4 nM, which is averaged from two independent measurements. Thus, depletion of $Ca^{2+}$ weakens the binding of PTH(1-34)-FAM to PTH1R-ND. Nonetheless, this weakening effect is reversible. Addition of 15 mM of $Ca^{2+}$ after $Ca^{2+}$-depletion can restore the binding affinity (Supplementary Figure 5).

**Activation of G-protein by PTH1R-ND upon Binding to PTH(1-34).** In addition to ligand binding, we also examined G-protein activation. We studied activation of $G_s$ by PTH1R-ND upon binding to unlabeled PTH(1-34) using a non-hydrolyzable fluorescently labeled GTP analogue, BODIPY FL GTPγS (Figure 4a). The fluorescence of BODIPY FL GTPγS is quenched when it is in an aqueous solution, but fluorescence is restored when it binds to $G_s$. Hence, an increase in fluorescence intensity indicates activation of $G_s$. Figure 4b shows the time dependence of fluorescence intensity measured simultaneously in identical cuvettes in four sample slots of the fluorimeter. At $t$ = 0, a reaction mixture, containing PTH1R-ND (20 nM), $G_s$ (100 nM), and BODIPY FL GTPγS (100 nM) in Buffer A, is aliquoted in each of the four slots. At $t \approx 6$ min, one of the following four solutions are added into each sample slot: (1) PTH(1-34) with addition of 15 mM $Ca^{2+}$, (2) PTH(1-34) with addition of 5 mM $Ca^{2+}$, (3) PTH(1-34) without addition of $Ca^{2+}$, and (4) the buffer. Then, the fluorescence intensity was monitored for ~3 h. The concentration of PTH(1-34) was fixed at 2 μM in all G-protein activity assays, which is expected to saturate the binding based on the measured $K_d$. Figure 4b shows the fluorescence signal continues to increase in the case of buffer alone, which represents the basal activity. Upon addition of PTH(1-34) in the presence of 5 or 15 mM $Ca^{2+}$, the fluorescence intensity further increases relative to the basal level. Such increase is larger for 15 mM than for 5 mM. Surprisingly, adding PTH(1-34) without a supplement of $Ca^{2+}$ causes a decrease of fluorescence signal relative to the basal level. Figure 4c shows the basal level subtracted fluorescence signal. When the buffer is supplemented with 5 and 15 mM of $Ca^{2+}$, addition of PTH(1-34) induces a positive response, indicating that PTH(1-34) is an agonist. In contrast, when the buffer is not supplemented with $Ca^{2+}$, addition of PTH(1-34) leads to a negative response, indicating that PTH(1-34) is an inverse agonist. These observations were made in five different experiments using independently prepared PTH1R-NDs.

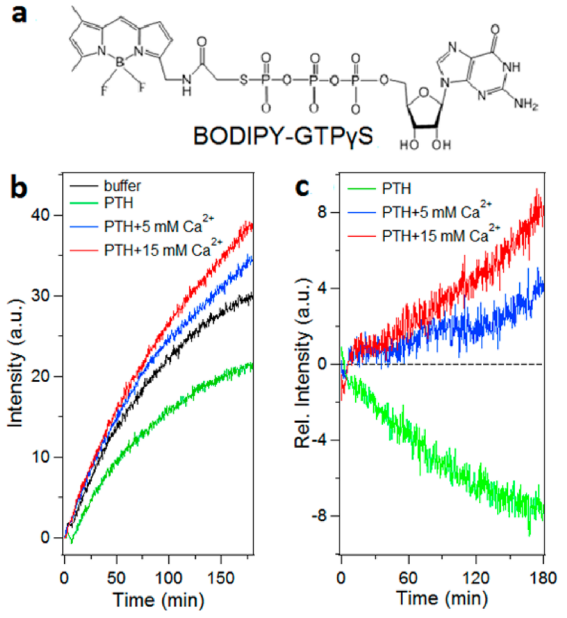


**Figure 4.** G-protein activity assay using BODIPY FL GTPγS. (a) Structure of nonhydrolyzable and fluorescently labeled BODIPY FL GTPγS. (b) Time-dependent BODIPY FL GTPγS fluorescence signal monitored simultaneously in 4 sample slots in a fluorimeter. At $t$ = 0, each sample slot contains a mixture of PTH1R-ND (20 nM), $G_s$ (100 nM), and BODIPY FL GTPγS (100 nM) in Buffer A; at $t \approx 6$ min, one of the following four solutions are added to each sample slot: (black) buffer, (green) 2 μM PTH(1-34), (blue) 2 μM PTH(1-34) with 5 mM $Ca^{2+}$, and (red) 2 μM PTH(1-34) with 15 mM $Ca^{2+}$. (c) Basal level or buffer subtracted time-dependent fluorescence signals. Buffer A: 20 mM Tris (pH 7.4), 150 mM NaCl, 100 μM EDTA, and 3 mM $MgCl_2$.

**Control Experiments.** To confirm that the G-protein activity and $Ca^{2+}$ effect shown in Figure 4 are specific to PTH1R, we performed control experiments where we replaced PTH1R-ND with empty-ND and examined the G-protein activity in response to addition of $Ca^{2+}$ and empty-NDs. At $t$ = 0, a mixture of $G_s$ (100 nM) and BODIPY FL GTPγS (100 nM) is aliquoted into two sample slots, and the fluorescence intensities are monitored simultaneously (Figure 5). In the first 45 min, the fluorescence signals remain unchanged, suggesting that $G_s$ exhibits no basal activity by itself. At $t \approx 45$ min, 15 mM $Ca^{2+}$ is added to slot 1 while Buffer A is added to slot 2. The fluorescence signals of the two samples stay the same for another 45 min, suggesting that BODIPY-GTPγS does not bind to $G_s$ and that $Ca^{2+}$ cannot activate $G_s$ in the absence of


dx.doi.org/10.1021/cb300466n | ACS Chem. Biol. 2013, 8, 617–625

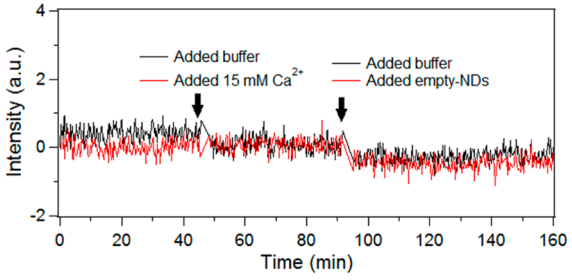


**Figure 5.** Control experiment: G-protein activity in the absence of PTH1R. At $t$ = 0, two sample slots of the fluorimeter contain the reaction mixture of $G_s$ (100 nM) and BODIPY FL GTPγS (100 nM) in Buffer A. At $t \approx 45$ min, 15 mM $Ca^{2+}$ is added to cuvette 1 (red), while Buffer A is added to cuvette 2 (black). At $t \approx 90$ min, 20 nM (final concentration) of empty-ND is added to cuvette 1 (red), while plain buffer is added to cuvette 2 (black). The fluorescence remains unchanged except decreases due to dilution.

PTH1R-ND. At $t \approx 90$ min, empty-ND is added to slot 1 while Buffer A is added to slot 2. The fluorescence intensity is monitored for an additional 70 min. Aside from the initial drop in signal due to dilution, the fluorescence intensity does not change, indicating that empty-NDs cannot activate $G_s$. We repeated these control experiments twice and made the same observations. We conclude that the observed $G_s$ activity (Figure 4) is specific to PTH1R and that the effect of $Ca^{2+}$ on the G-protein activity (Figure 4) is exerted through the purified PTH1R-ND.

**Residual $Ca^{2+}$ Required for Basal PTH1R Activity.** To test whether residual $Ca^{2+}$ in buffer is important for G-protein activity, we performed the same G-protein activity assay under a $Ca^{2+}$-depleting condition (200 μM EGTA) (Figure 6a). At $t$ = 0, the three sample slots in the fluorimeter are filled with the same mixture of PTH1R-ND, $G_s$, and BODIPY FL GTPγS. At $t \approx 15$ min, one of the following solutions are added to each sample: (1) 2 μM PTH(1-34), (2) 2 μM PTH(1-34) with 200 μM EGTA, and (3) 2 μM PTH(1-34) with 5 mM $Ca^{2+}$ (specified as final concentrations). Addition of PTH(1-34) in the presence of EGTA gives a small fluorescence response, suggesting that PTH(1-34) can barely activate G-protein *via* PTH1R-ND under the $Ca^{2+}$-depleting condition. In contrast, addition of PTH(1-34) in the absence of EGTA results in an increase in fluorescence signal. The presence of 15 mM $Ca^{2+}$ produces a more robust increase in signal than when no $Ca^{2+}$is added. Moreover, we tested the effect of depletion of $Ca^{2+}$ on the basal activity, *i.e.*, in the absence of the ligand. Figure 6b shows that after two solutions, (1) Buffer A and (2) Buffer A with 200 μM EGTA, are added, the increase in fluorescence signal is greater in the absence of EGTA than in the presence of EGTA. The results suggest that residual $Ca^{2+}$ in the buffer is important for the basal activity of PTH1R-ND.

**$Ca^{2+}$ Alone As a Weak Agonist of PTH1R.** We further compared the effect of PTH(1-34) and $Ca^{2+}$ on activating G-protein *via* PTH1R-ND (Figure 6c). To the same mixture of PTH1R-ND, $G_s$, and BODIPY FL GTPγS, in three sample slots of the fluorimter, we added one of the following three solutions: (1) 2 μM PTH(1-34) with 5 mM $Ca^{2+}$, (2) 5 mM $Ca^{2+}$, and (3) Buffer A, all mentioned as final concentrations. Addition of 5 mM $Ca^{2+}$ in the absence of PTH(1-34) leads to a greater increase in fluorescence relative to buffer alone, suggesting that $Ca^{2+}$ alone can activate G-protein in the presence of PTH1R-ND. However, this increase is much less than when both $Ca^{2+}$ and PTH(1-34) are present. This result reveals that $Ca^{2+}$ by itself can act as an agonist under our experimental conditions, but the effect is relatively weak when compared with PTH(1-34) in the presence of $Ca^{2+}$.

## DISCUSSION

We have established a nanodisc-based protocol to purify a family B GPCR, PTH1R. This protocol incorporates PTH1R into nanodiscs immediately after membrane solubilization to avoid prolonged contact with detergents. Once in nanodiscs, PTH1R is isolated by single-step affinity purification (Figure 1). Also, we have developed functional assays to detect ligand binding and G-protein activation. Ligand binding was detected with a fluorescently labeled ligand using fluorescence anisotropy, and G-protein activity was examined using a

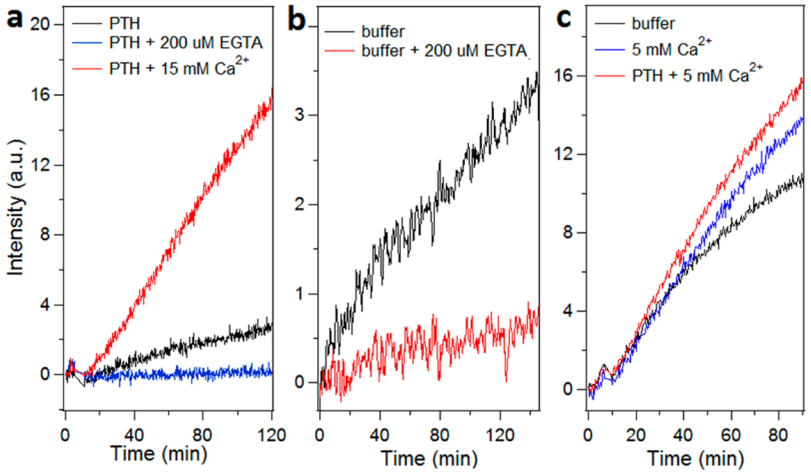


**Figure 6.** Calcium-dependent G-protein activity. Time-dependent BODIPY FL GTPγS fluorescence signal monitored simultaneously in 2 or 3 sample slots in a fluorimeter. At $t$ = 0, each sample slot contains PTH1R-ND (20 nM), $G_s$ (100 nM), and BODIPY FL GTPγS (100 nM) in Buffer A. (a) At $t \approx 15$ min, one of the following three solutions are added to each sample slot: (black —) 2 μM PTH(1-34), (blue —) 2 μM PTH(1-34) with 200 μM EGTA, and (red —) 2 μM PTH(1-34) with 15 mM $Ca^{2+}$. (b) At $t \approx 6$ min, two solutions are added to 2 sample slots: (black —) buffer and (red —) buffer with 200 μM EGTA. (c) At $t$ = 8 min, one of the three solutions are added to each of the three sample slots: (black —) buffer, (blue —) 5 mM $Ca^{2+}$, and (red —) 2 μM PTH(1-34) with 5 mM $Ca^{2+}$(specified as final concentrations).


dx.doi.org/10.1021/cb300466n | ACS Chem. Biol. 2013, 8, 617–625

nonhydrolyzable fluorescently labeled GTP analogue. Using these assays, we confirmed signal transduction activity of the purified PTH1R-ND. We also showed that $Ca^{2+}$ has a profound effect on the signal transduction activity of purified PTH1R-ND under our experimental conditions. Addition of 15 mM $Ca^{2+}$ enhanced the binding of PTH(1-34) to PTH1R-ND by a factor of 17 ± 4, in comparison to when experiment was done in the presence of residual $Ca^{2+}$, *i.e.*, without addition of EGTA, and by a factor of 24 ± 5 in comparison to when experiment was done in the absence of any $Ca^{2+}$, *i.e.*, in the presence of 200 $\mu$M EGTA. Moreover, $Ca^{2+}$ by itself was able to act as a weak agonist for PTH1R-ND to activate $G_s$. Unexpectedly, PTH(1-34) behaved as an inverse agonist when no additional $Ca^{2+}$ was present but supplementing with millimolar amounts (5 or 15 mM) of $Ca^{2+}$ switched PTH(1-34) to an agonist under our experimental conditions.

Our observations of the effect of $Ca^{2+}$ on the signaling process of PTH1R in nanodiscs generate a number of important questions: What is the molecular mechanism of the $Ca^{2+}$ effect? How does $Ca^{2+}$ change the structure and dynamics of PTH1R in both micromolar and millimolar concentration? How do these changes in PTH1R alter ligand binding and G-protein activation? What is the physiological relevance of $Ca^{2+}$ on PTH1R signaling in modulating $Ca^{2+}$ homeostasis? While PTH(1-34) is known to trigger bone resorption (release of $Ca^{2+}$ from bone), intermittent injection of PTH(1-34) is a treatment for osteoporosis. Could the observed effect of $Ca^{2+}$ on the PTH1R signaling process provide molecular insights into the pharmacological efficacy of the PTH(1-34) treatment? As for now, all of these questions remain unanswered. However, we have started exploring some of them.

We hypothesized that $Ca^{2+}$ can alter the secondary structure of PTH(1-34) in solution to enhance its binding to PTH1R-ND. Previous studies have shown that many peptide ligands of family B GPCRs adopt $\alpha$-helical structures upon binding to the receptors but exhibit little or no secondary structure in solution.[43,44] PTH(1-34) is found to be partially helical in solution[45] but is crystallized as a full helix.[46] To test whether $Ca^{2+}$ could increase the $\alpha$-helical content in PTH(1-34) in solution and thereby enhance the binding, we acquired circular dichroism spectra of PTH(1-34) at 0−15 mM of $Ca^{2+}$. The spectra revealed the presence of both $\alpha$-helical and disordered structures (Supplementary Figure 6). No change in secondary structure was observed upon addition of $Ca^{2+}$. Hence, $Ca^{2+}$ does not promote formation of $\alpha$-helical structure in PTH(1-34) to enhance binding.

Our results show that $Ca^{2+}$ at a concentration of 15 mM can alter the affinity of PTH(1-34) toward PTH1R-ND and the G-protein activity of PTH1R-ND. Nonetheless, the $Ca^{2+}$ concentration in blood is strictly regulated at ∼2.5 mM, of which only half exists as free ions.[47] However, local $Ca^{2+}$ concentrations in the extracellular fluid around osteoblasts, bone cells that express PTH1R, can be momentarily boosted up to ∼40 mM during the bone resorption process.[48] It would be interesting to test whether this instantaneous increase in $Ca^{2+}$ concentration to millimolar levels at the osteoblasts *in vivo* could further mediate bone resorption *via* PTH1R signaling.

Moreover, the effects of $Ca^{2+}$ on the signaling activity of PTH1R-ND imply that there could be $Ca^{2+}$ binding site(s) on the receptor and/or that $Ca^{2+}$ can alter protein dynamics and shift PTH1R to a more active-like conformation. When residual $Ca^{2+}$ is removed from the buffer by EGTA, PTH1R-ND can barely activate G-protein both in the presence and absence of ligand. The effect of millimolar levels of $Ca^{2+}$ on both ligand binding and $G_s$ activity also points toward interactions of $Ca^{2+}$ with PTH1R and/or the signaling complex, PTH(1-34)-PTH1R-ND-$G_s$. We are in the process of building homology models in conjunction with mutagenesis to explore the possibility of identifying the $Ca^{2+}$-binding site(s).

An important factor that might contribute toward the behavior of any membrane protein is the composition of lipids in the bilayer in its immediate vicinity. A recent study on the family A GPCR neurotensin receptor 1 (NTR1) in nanodiscs has demonstrated that although this receptor binds to its ligand independently of lipid composition in the lipid bilayer, its interaction with the G-protein, $G_q$, is determined by whether the nanodisc is composed exclusively of zwitterionic POPC or a mixture of POPC and the negatively charged POPG (1-palmitoyl-2-oleoyl-*sn*-glycero-3-phospho-(1′-*rac*-glycerol)).[49] Increasing the proportion of the negatively charged POPG resulted in increased affinity for $G_q$, as well as increased nucleotide exchange rates. Similarly, by increasing the ratio of negatively charged POPS (1-palmitoyl-2-oleoyl-*sn*-glycero-3-phospho-L-serine) to POPC, rhodopsin incorporated in nanodiscs showed increased association with arrestin-1.[28]

In this manuscript, we have used POPC alone to make nanodiscs. Taking into account the lipid contribution from the cell membrane, we will have only ∼7% non-POPC lipids in the nanodiscs (see Supplementary Results for estimation). It is quite likely that upon changing the lipid content of the PTH1R-ND bilayer to where we have significant amounts of negatively charged lipids, such as POPG or POPS, we will observe an increased association of PTH1R-ND with the $G_s$ trimer. We plan to perform further experiments by varying the lipid content of the nanodisc bilayer to observe any changes in the association of G-protein with PTH1R.

The existence of GPCR oligomers and consequences of these oligomers on GPCR function have been under intense study for some time. The ability to control the number of receptor/GPCR molecules in the nanodisc makes them an important tool for the study of the effect of receptor oligomerization on ligand binding and signal transduction. Using nanodiscs, it has been shown that GPCRs such as rhodopsin,[28,29,50] $\beta_2$-adrenergic receptor,[25] neurotensin,[49] and $\mu$-opioid receptor[27] monomers are sufficient for functional association with G-protein. In fact, monomeric rhodopsin in nanodiscs is also shown to undergo phosphorylation by rhodopsin kinase (GRK1) and bind with arrestin-1.[28]

FRET (fluorescence resonance energy transfer) and BRET (bioluminescence resonance energy transfer) studies in live cells have shown that in the absence of bound ligand, PTH1R can exist as a dimer in the cell membrane,[51] but this does not necessarily imply that PTH1R solubilized from cell membranes using detergents will continue to exist as a dimer in the resulting micelles. For instance, $\beta_2$-adrenergic receptor has been shown to dimerize in the cell membrane[52] but is found to be a monomer in detergent micelles after solubilization,[25] *i.e.*, the dimer does not survive the high concentration of detergent. Thus, it is likely that PTH1R also forms monomers in detergent micelles and exists in the monomeric state in the nanodisc as well. In the future, we plan to carry out experiments to determine the oligimerization status of PTH1R in nanodiscs and understand the function of the receptor with respect to its oligimerization status.

In conclusion, we have established a method to purify the family B GPCR PTH1R in nanodiscs and developed functional assays to examine ligand binding and G-protein activity of the protein. The ligand binding assays can be adapted to other family B GPCRs, while the G-protein activity assay can be generally applied to other GPCRs. Our nanodisc-based method enables biochemical and functional characterization of the receptor in the absence of interfering factors from the cell or membrane preparations, including various interacting proteins and feedback regulations, facilitating our observation of the profound effects of $Ca^{2+}$ on the signaling process of PTH1R. The observations lead to a number of questions that introduce opportunities for further research on PTH1R's function. The purification method yields the receptor directly into nanodiscs, which could be an ideal platform for biophysical characterization, such as single-molecule spectroscopy and electron paramagnetic resonance spectroscopy. Such studies can potentially reveal a detailed activation mechanism in terms of conformational changes in the transmembrane region, which has remained almost unknown for family B GPCRs. The purification method utilizing nanodiscs can be readily tested and optimized for all other GPCRs with minimum adaptations and can theoretically be extended to other integral membrane proteins, potentially yielding a general method for purifying transmembrane proteins that cannot be purified in detergent systems.

## METHODS

**Materials.** Three peptides were synthesized at the Keck Biotechnology Resource Laboratory at Yale University: 1D5 peptide (TETSQVAPA), PTH(1-34), and PTH(1-34)FAM, *i.e.*, PTH(1-34) conjugated to 5(6)-carboxyfluorescein at Lys 13 (Figure 3a). BODIPY FL GTPγS (Figure 4a) was purchased from Invitrogen. Membrane scaffold protein (MSP1E3D1) was expressed and purified as described previously[14] with minor modifications (see Supplementary Methods). The lipid 1-palmitoyl-2-oleoyl-*sn*-glycero-3-phosphocholine (POPC) was obtained from Avanti Polar Lipids, and the detergent *n*-dodecyl-β-D-maltopyranoside (DDM) was from Anatrace. All other chemicals were analytical grade obtained from Sigma or American Biochemicals.

**Expression of Human PTH1R in HEK293 Cells.** The human PTH1R was expressed with a 1D5 tag (TETSQVAPA) at its C-terminus, in the tetracycline-inducible vector pACMV-tetO in HEK293S *GnTI*$^-$ cells.[53,54] Details of the plasmid construction and cell line generation are described in Supplementary Methods. PTH1R stable cells were induced with 0.55 mg/mL sodium butyrate and 2 μg/mL tetracycline and maintained under 5% $CO_2$/95% air atmosphere in 1:1 DMEM/F12 supplemented with 10% FBS. After 48 h, membrane fractions were isolated as described in Supplementary Methods.

**Nanodisc Assembly.** Preparations of solubilized POPC, MSP1E3D1, and the membrane fraction pellet of the HEK293 cells are described in detail in Supplementary Methods. The pellet from about 45−60 10-cm plates was resuspended in 600 μL of Solubilization Buffer (50 mM Tris pH 7.4, 150 mM NaCl, 5 mM $CaCl_2$, 5 mM $MgCl_2$, 2 mM EDTA, 10% glycerol, and 0.5% DDM) in the presence of Protease Inhibitor Cocktail Set III (EMD Biosciences) for 1 h at 4 °C and then spun at 15,000 × *g* for 15 min. The supernatant was quantified for total protein using the Pierce BCA protein assay kit (Thermo Scientific). Using an average MW of 40,000 for membrane proteins,[55] the protein concentration was calculated. The nanodiscs were assembled in multiple 1.5 mL centrifuge tubes in a final volume of 400 μL of assembly mixture per tube. The concentration of the different components were 90 μM MSP1E3D1, 8 mM POPC, and 180 μg (~11 μM) of total membrane protein made up to a final volume in a buffer containing 50 mM Tris pH 7.4, 150 mM NaCl, 5 mM $MgCl_2$, 5 mM $CaCl_2$, 4 mM EDTA, and 4% glycerol. The nanodisc assembly mix was incubated on ice for 45 min and then transferred into another 1.5 mL centrifuge tube containing 150 mg of washed Bio-Beads SM-2 (Bio-Rad) to initiate nanodisc formation. The mixture was gently mixed overnight at 4 °C. Next morning, the assembled nanodiscs were affinity purified as detailed in Supplementary Methods.

**Expression and Purification of $G_s$ Heterotrimer.** $G_s$ heterotrimer was expressed and purified exactly as described previously.[9] Briefly, bovine $G_{\alpha s}$ short, His6-rat $G_{\beta 1}$, and bovine $G_{\gamma 2}$ were expressed together as the heterotrimer in HighFive insect cells and solublized with sodium cholate. The protein was exchanged into DDM detergent and purified by using Ni-NTA, Mono-Q, and Superdex 200 chromatography.

**Size Exclusion Chromatography.** Purified PTH1R-containing nanodiscs were resolved using a Superdex 200 10/300 GL column at a flow rate of 0.4 mL/min. Five protein standards were used to calibrate the column: thyroglobulin (17.2 nm), apoferritin (12.2 nm), alcohol dehydrogenase (9.1 nm), bovine serum albumin (7.2 nm), and carbonic anhydrase (4 nm).

**Electron Microscopy.** A 4 μL of sample at 80 nM was applied to a glow-discharged carbon-coated EM grid and negatively stained with 2% uranyl acetate (w/v) solution. The specimen was subsequently examined in a FEI Tecnai-12 electron microscope operated at 120 kV. Images were collected as 4096 × 4096-pixel 8-bit gray scale Gatan Digital Micrograph 3 (DM3) files on a Gatan Ultrascan 4000 CCD camera at 52,000×. Particle sizes were estimated using Eman2.

**Ligand Binding Assays.** The binding between PTH and PTH1R-ND was determined by fluorescence anisotropy using PTH(1-34)-FAM. We confirmed that this FAM-labeled peptide was able to bind PTH1R on PTH1R-expressing cells using flow cytometry (see Supporting Information). In our binding assay shown in Figure 2, a 50 nM solution of PTH(1-34)-FAM was incubated with different concentrations of nanodiscs in a buffer containing 20 mM Tris-HCl, pH 7.4, 150 mM NaCl, 100 μM EDTA, 3 mM $MgCl_2$, and with $CaCl_2$ concentration as indicated. Titration using empty nanodiscs under the same conditions was set up as a control experiment. The measurements were made on a PTI QuantaMaster C-61 two-channel fluorescence spectrophotometer with excitation (497 nm) and emission (518 nm) slit widths of 5 nm. The ligand was mixed with PTH1R nanodiscs in a cuvette; the entire sample in the cuvette was pipetted up and down 3−4 times for through mixing and then incubated for one minute. The anisotropy was averaged over 60 s with one reading per second. All experiments were performed at 30 °C. Anisotropy was measured before and after adding $CaCl_2$ to the cuvette, with a 1-min wait after adding calcium. Anisotropy data were fitted using eq 1 with three fitting parameters $K_d$, $r_b$, and $r_f$ (see Supporting Information). The value of $r_b$ obtained from the data fitted in the presence of calcium was used for fitting in the calcium free condition.

**G-Protein Activation Assay.** We measured $G_s$ activation using BODIPY FL GTPγS, whose fluorescence intensity increases upon binding to the G-protein. The G-protein association with BODIPY-GTPγS was monitored using a fluorescence spectrophotometer (Cary Eclipse, Varian Inc.) with a multicell peltier block, with 2.5 nm excitation (500 nm) and 5 nm emission (511 nm) slit widths at 30 °C. Reaction buffer (20 mM Tris-HCl, pH 7.4, 150 mM NaCl, 100 μM EDTA, 3 mM $MgCl_2$), 100 nM $G_s$, 100 nM BODIPY-GTPγS, and 20 nM PTH1R nanodisc were added in a cuvette to a final volume of 54 μL. Fluorescence was monitored for about six minutes before addition of 6 μL of either PTH(1-34) alone to a final concentration of 2 μM or PTH(1-34) with $CaCl_2$ at 5 or 15 mM final concentration. Stock solutions of all reagents in the reaction were made in reaction buffer except for $G_s$, which was diluted in 0.2% DDM used to stabilize the G-protein. The final reaction mixture, containing 78 μM DDM, was found to have no effect on the stability of nanodiscs within the time scale of the G-protein activity assay (see Supporting Information).

## ASSOCIATED CONTENT

### Supporting Information

This material is available free of charge *via* the Internet at http://pubs.acs.org.


dx.doi.org/10.1021/cb300466n | *ACS Chem. Biol.* 2013, 8, 617−625

## AUTHOR INFORMATION


### Corresponding Author

*E-mail: elsa.yan@yale.edu.

### Author Contributions

§These authors contributed equally to this work.


### Notes

The authors declare no competing financial interest.

## ACKNOWLEDGMENTS

The authors would like to thank J. Wysolmerski, C. Crews, V. Batista, I. Rivalta, Y. Guo, and L. Fu (Yale University) for useful discussions and X. Li for assistance in the experiments. We thank H. Wang (Yale University), currently at Tsinghua University (PR China), for the help with electron microscopy imaging. We thank P. Reeves (University of Essex) for providing the pACMV-*tet*O vector and HEK293S *GnTI*$^-$ cells. N.M. acknowledges support from the Seessel Postdoctoral Fellowship, and J.L. acknowledges the support from the Anderson Postdoctoral Fellowship. V.M. is the recipient of the National Science Foundation fellowship (DGE-0644492), and E.S. was the recipient of the Yale-HHMI Future Scientist Fellowship and the Sackler Undergraduate Fellowship. E.Y. is the recipient of the NSF CAREER Award. This work was supported by the Yale Setup Fund.

## REFERENCES


(1) Schioth, H. B., and Lagerstrom, M. C. (2008) Structural diversity of G protein-coupled receptors and significance for drug discovery. *Nat. Rev. Drug Discov. 7*, 339−357.

(2) Fredriksson, R., Lagerstrom, M. C., Lundin, L. G, and Schioth, H. B. (2003) The G-protein-coupled receptors in the human genome form five main families. Phylogenetic analysis, paralogon groups, and fingerprints. *Mol. Pharmacol. 63*, 1256−1272.

(3) Hofmann, K. P., Scheerer, P., Hildebrand, P. W., Choe, H. W., Park, J. H., Heck, M., and Ernst, O. P. (2009) A G protein-coupled receptor at work: the rhodopsin model. *Trends Biochem. Sci. 34*, 540−552.

(4) Altenbach, C., Kusnetzow, A. K., Ernst, O. P., Hofmann, K. P, and Hubbell, W. L. (2008) High-resolution distance mapping in rhodopsin reveals the pattern of helix movement due to activation. *Proc. Natl. Acad. Sci. U.S.A. 105*, 7439−7444.

(5) Ghanouni, P., Steenhuis, J. J., Farrens, D. L, and Kobilka, B. K. (2001) Agonist-induced conformational changes in the G-protein-coupling domain of the beta 2 adrenergic receptor. *Proc. Natl. Acad. Sci. U.S.A. 98*, 5997−6002.

(6) Yao, X., Parnot, C., Deupi, X., Ratnala, V. R., Swaminath, G., Farrens, D., and Kobilka, B. (2006) Coupling ligand structure to specific conformational switches in the beta2-adrenoceptor. *Nat. Chem. Biol. 2*, 417−422.

(7) Standfuss, J., Edwards, P. C., D'Antona, A., Fransen, M., Xie, G., Oprian, D. D, and Schertler, G. F. (2011) The structural basis of agonist-induced activation in constitutively active rhodopsin. *Nature 471*, 656−660.

(8) Rasmussen, S. G. F., Choi, H. J., Fung, J. J., Pardon, E., Casarosa, P., Chae, P. S., DeVree, B. T., Rosenbaum, D. M., Thian, F. S., Kobilka, T. S., Schnapp, A., Konetzki, I., Sunahara, R. K., Gellman, S. H., Pautsch, A., Steyaert, J., Weis, W. I, and Kobilka, B. K. (2011) Structure of a nanobody-stabilized active state of the beta(2) adrenoceptor. *Nature 469*, 175−180.

(9) Rasmussen, S. G., Devree, B. T., Zou, Y., Kruse, A. C., Chung, K. Y., Kobilka, T. S., Thian, F. S., Chae, P. S., Pardon, E., Calinski, D., Mathiesen, J. M., Shah, S. T., Lyons, J. A., Caffrey, M., Gellman, S. H., Steyaert, J., Skiniotis, G., Weis, W. I., Sunahara, R. K, and Kobilka, B. K. (2011) Crystal structure of the beta(2) adrenergic receptor-Gs protein complex. *Nature 477*, 549−555.

(10) Grisshammer, R. (2009) Purification of recombinant G-protein-coupled receptors. *Methods Enzymol. 463*, 631−645.

(11) Serebryany, E., Zhu, G. A, and Yan, E. C. Y. (2012) Artificial membrane-like environments for in vitro studies of purified G-protein coupled receptors. *Biochim. Biophys. Acta, Biomembr. 1818*, 225−233.

(12) Sakmar, T. P., Banerjee, S., and Huber, T. (2008) Rapid incorporation of functional rhodopsin into nanoscale apolipoprotein bound bilayer (NABB) particles. *J. Mol. Biol. 377*, 1067−1081.

(13) Denisov, I. G., Grinkova, Y. V., Lazarides, A. A, and Sligar, S. G. (2004) Directed self-assembly of monodisperse phospholipid bilayer Nanodiscs with controlled size. *J. Am. Chem. Soc. 126*, 3477−3487.

(14) Sligar, S. G., Bayburt, T. H, and Grinkova, Y. V. (2002) Self-assembly of discoidal phospholipid bilayer nanoparticles with membrane scaffold proteins. *Nano Lett. 2*, 853−856.

(15) Orwick, M. C., Judge, P. J., Procek, J., Lindholm, L., Graziadei, A., Engel, A., Grobner, G., and Watts, A. (2012) Detergent-free formation and physicochemical characterization of nanosized lipid-polymer complexes: Lipodisq. *Angew. Chem., Int. Ed. 51*, 4653−4657.

(16) Bayburt, T. H, and Sligar, S. G. (2003) Self-assembly of single integral membrane proteins into soluble nanoscale phospholipid bilayers. *Protein Sci. 12*, 2476−2481.

(17) Boldog, T., Grimme, S., Li, M., Sligar, S. G, and Hazelbauer, G. L. (2006) Nanodiscs separate chemoreceptor oligomeric states and reveal their signaling properties. *Proc. Natl. Acad. Sci. U.S.A. 103*, 11509−11514.

(18) Denisov, I. G., Baas, B. J., Grinkova, Y. V, and Sligar, S. G. (2007) Cooperativity in cytochrome P450 3A4: linkages in substrate binding, spin state, uncoupling, and product formation. *J. Biol. Chem. 282*, 7066−7076.

(19) Knepp, A. M., Grunbeck, A., Banerjee, S., Sakmar, T. P, and Huber, T. (2011) Direct measurement of thermal stability of expressed CCR5 and stabilization by small molecule ligands. *Biochemistry 50*, 502−511.

(20) Ranaghan, M. J., Schwall, C. T., Alder, N. N, and Birge, R. R. (2011) Green proteorhodopsin reconstituted into nanoscale phospholipid bilayers (nanodiscs) as photoactive monomers. *J. Am. Chem. Soc. 133*, 18318−18327.

(21) Yan, R., Mo, X., Paredes, A. M., Dai, K. S., Lanza, F., Cruz, M. A, and Li, R. H. (2011) Reconstitution of the platelet glycoprotein Ib-IX complex in phospholipid bilayer nanodiscs. *Biochemistry 50*, 10598−10606.

(22) Li, M. S, and Hazelbauer, G. L. (2011) Core unit of chemotaxis signaling complexes. *Proc. Natl. Acad. Sci. U.S.A. 108*, 9390−9395.

(23) Shi, L., Shen, Q. T., Kiel, A., Wang, J., Wang, H. W., Melia, T. J., Rothman, J. E, and Pincet, F. (2012) SNARE proteins: one to fuse and three to keep the nascent fusion pore open. *Science 335*, 1355−1359.

(24) Ritchie, T. K., Grinkova, Y. V., Bayburt, T. H., Denisov, I. G., Zolnerciks, J. K., Atkins, W. M, and Sligar, S. G. (2009) Reconstitution of membrane proteins in phospholipid bilayer nanodiscs. *Methods Enzymol. 464*, 211−231.

(25) Whorton, M. R., Bokoch, M. P., Rasmussen, S. G., Huang, B., Zare, R. N., Kobilka, B., and Sunahara, R. K. (2007) A monomeric G protein-coupled receptor isolated in a high-density lipoprotein particle efficiently activates its G protein. *Proc. Natl. Acad. Sci. U.S.A. 104*, 7682−7687.

(26) Whorton, M. R., Jastrzebska, B., Park, P. S., Fotiadis, D., Engel, A., Palczewski, K., and Sunahara, R. K. (2008) Efficient coupling of transducin to monomeric rhodopsin in a phospholipid bilayer. *J. Biol. Chem. 283*, 4387−4394.

(27) Kuszak, A. J., Pitchiaya, S., Anand, J. P., Mosberg, H. I., Walter, N. G, and Sunahara, R. K. (2009) Purification and functional reconstitution of monomeric mu-opioid receptors: allosteric modulation of agonist binding by Gi2. *J. Biol. Chem. 284*, 26732−26741.

(28) Bayburt, T. H., Vishnivetskiy, S. A., McLean, M. A., Morizumi, T., Huang, C. C., Tesmer, J. J., Ernst, O. P., Sligar, S. G, and Gurevich, V. V. (2011) Monomeric rhodopsin is sufficient for normal rhodopsin kinase (GRK1) phosphorylation and arrestin-1 binding. *J. Biol. Chem. 286*, 1420−1428.

(29) Tsukamoto, H., Sinha, A., DeWitt, M., and Farrens, D. L. (2010) Monomeric rhodopsin is the minimal functional unit required for arrestin binding. *J. Mol. Biol. 399*, 501−511.
(30) Civjan, N. R., Bayburt, T. H., Schuler, M. A., and Sligar, S. G. (2003) Direct solubilization of heterologously expressed membrane proteins by incorporation into nanoscale lipid bilayers. *Biotechniques 35*, 556−560.
(31) Ohtaki, T., Masuda, Y., Ishibashi, Y., Kitada, C., Arimura, A., and Fujino, M. (1993) Purification and characterization of the receptor for pituitary adenylate cyclase-activating polypeptide. *J. Biol. Chem. 268*, 26650−26657.
(32) Ohtaki, T., Ogi, K., Masuda, Y., Mitsuoka, K., Fujiyoshi, Y., Kitada, C., Sawada, H., Onda, H., and Fujino, M. (1998) Expression, purification, and reconstitution of receptor for pituitary adenylate cyclase-activating polypeptide - large-scale purification of a functionally active G protein-coupled receptor produced in Sf9 insect cells. *J. Biol. Chem. 273*, 15464−15473.
(33) Segre, G. V., Shimada, M., Chen, X., Cvrk, T., Hilfiker, H., and Parfenova, M. (2002) Purification and characterization of a receptor for human parathyroid hormone and parathyroid hormone-related peptide. *J. Biol. Chem. 277*, 31774−31780.
(34) Gan, L., Alexander, J. M., Wittelsberger, A., Thomas, B., and Rosenblatt, M. (2006) Large-scale purification and characterization of human parathyroid hormone-1 receptor stably expressed in HEK293S GnTI- cells. *Protein Expression Purif. 47*, 296−302.
(35) Michalke, K., Huyghe, C., Lichiere, J., Graviere, M. E., Siponen, M., Sciara, G., Lepaul, I., Wagner, R., Magg, C., Rudolph, R., Cambillau, C., and Desmyter, A. (2010) Mammalian G protein-coupled receptor expression in Escherichia coli: II. refolding and biophysical characterization of mouse cannabinoid receptor 1 and human parathyroid hormone receptor 1. *Anal. Biochem. 401*, 74−80.
(36) Schroder-Tittmann, K., Bosse-Doenecke, E., Reedtz-Runge, S., Ihling, C., Sinz, A., Tittmann, K., and Rudolph, R. (2010) Recombinant expression, in vitro refolding, and biophysical characterization of the human glucagon-like peptide-1 receptor. *Biochemistry 49*, 7956−7965.
(37) Tsang, C., Grihalde, N., Korepanova, A., Lake, M., Pereda-Lopez, A., Reilly, R. M., Walter, K., and Chiu, M. (2006) BIOT 138-Expression and purification of the glucagon-like peptide-1 receptor, *Abstracts of Papers of the 232nd ACS National Meeting, San Francisco*, The American Chemical Society, Washington, DC.
(38) Klammt, C., Perrin, M. H., Maslennikov, I., Renault, L., Krupa, M., Kwiatkowski, W., Stahlberg, H., Vale, W., and Choe, S. (2011) Polymer-based cell-free expression of ligand-binding family B G-protein coupled receptors without detergents. *Protein Sci. 20*, 1030−1041.
(39) Mannstadt, M., Juppner, H., and Gardella, T. J. (1999) Receptors for PTH and PTHrP: their biological importance and functional properties. *Am. J. Physiol.: Renal 277*, F665−F675.
(40) Kronenberg, H. M. (2006) PTHrP and skeletal development. *Ann. N.Y. Acad. Sci. 1068*, 1−13.
(41) Wysolmerski, J. J., Philbrick, W. M., Dunbar, M. E., Lanske, B., Kronenberg, H., Karaplis, A., and Broadus, A. E. (1998) Rescue of the parathyroid hormone-related protein knockout mouse demonstrates that parathyroid hormone-related protein is essential for mammary gland development. *Development 125*, 1285−1294.
(42) Jilka, R. L. (2007) Molecular and cellular mechanisms of the anabolic effect of intermittent PTH. *Bone 40*, 1434−1446.
(43) Parthier, C., Reedtz-Runge, S., Rudolph, R., and Stubbs, M. T. (2009) Passing the baton in class B GPCRs: peptide hormone activation via helix induction? *Trends Biochem. Sci. 34*, 303−310.
(44) Pioszak, A. A., and Xu, H. E. (2011) Molecular recognition of parathyroid hormone by its G protein-coupled receptor. *Prot. Natl. Acad. Sci. U.S.A. 105*, 5034−5039.
(45) Marx, U. C., Adermann, K., Bayer, P., Forssmann, W. G, and Rosch, P. (2000) Solution structures of human parathyroid hormone fragments hPTH(1-34) and hPTH(1−39) and bovine parathyroid hormone fragment bPTH(1−37). *Biochem. Biophys. Res. Commun. 267*, 213−220.
(46) Jin, L., Briggs, S. L., Chandrasekhar, S., Chirgadze, N. Y., Clawson, D. K., Schevitz, R. W., Smiley, D. L., Tashjian, A. H, and Zhang, F. (2000) Crystal structure of human parathyroid hormone 1-34 at 0.9-A resolution. *J. Biol. Chem. 275*, 27238−27244.
(47) Talmage, D. W, and Talmage, R. V. (2007) Calcium homeostasis: how bone solubility relates to all aspects of bone physiology. *J. Musculoskeletal Neuronal Interact. 7*, 108−112.
(48) Silver, I. A., Murrills, R. J, and Etherington, D. J. (1988) Microelectrode studies on the acid microenvironment beneath adherent macrophages and osteoclasts. *Exp. Cell. Res. 175*, 266−276.
(49) Inagaki, S., Ghirlando, R., White, J. F., Gvozdenovic-Jeremic, J., Northup, J. K, and Grisshammer, R. (2012) Modulation of the interaction between neurotensin receptor NTS1 and Gq protein by lipid. *J. Mol. Biol. 417*, 95−111.
(50) Bayburt, T. H., Leitz, A. J., Xie, G. F., Oprian, D. D, and Sligar, S. G. (2007) Transducin activation by nanoscale lipid bilayers containing one and two rhodopsins. *J. Biol. Chem. 282*, 14875−14881.
(51) Pioszak, A. A., Harikumar, K. G., Parker, N. R., Miller, L. J, and Xu, H. E. (2010) Dimeric arrangement of the Parathyroid hormone receptor and a structural mechanism for ligand-induced dissociation. *J. Biol. Chem. 285*, 12435−12444.
(52) Angers, S., Salahpour, A., Joly, E., Hilairet, S., Chelsky, D., Dennis, M., and Bouvier, M. (2000) Detection of beta(2)-adrenergic receptor dimerization in living cells using bioluminescence resonance energy transfer (BRET). *Proc. Natl. Acad. Sci. U.S.A. 97*, 3684−3689.
(53) Reeves, P. J., Kim, J. M, and Khorana, H. G. (2002) Structure and function in rhodopsin: a tetracycline-inducible system in stable mammalian cell lines for high-level expression of opsin mutants. *Proc. Natl. Acad. Sci. U.S.A. 99*, 13413−13418.
(54) Reeves, P. J., Callewaert, N., Contreras, R., and Khorana, H. G. (2002) Structure and function in rhodopsin: high-level expression of rhodopsin with restricted and homogeneous N-glycosylation by a tetracycline-inducible N-acetylglucosaminyltransferase I-negative HEK293S stable mammalian cell line. *Proc. Natl. Acad. Sci. U.S.A. 99*, 13419−13424.
(55) Muller, D. J., Wu, N., and Palczewski, K. (2008) Vertebrate membrane proteins: structure, function, and insights from biophysical approaches. *Pharmacol. Rev. 60*, 43−78.